

Tropical tropopause layer characteristics observed at different scales over the complete Indian region using INSAT-3D sounder measurements

A. Hemanth Kumar and M. Venkat Ratnam*

National Atmospheric Research Laboratory, Department of Space, Gadanki 517 112, India

Several studies were carried out for understanding the temporal variability of the tropopause characteristics using radiosonde measurements. This paper investigates the variability of tropopause characteristics using INSAT-3D temperature profiles. The seasonal mean of cold point tropopause temperature (CPT) and corresponding pressure (CPH), convective tropopause temperature (COT) and corresponding pressure (COH) obtained from the hourly temperature profiles of the INSAT-3D represents the actual seasonal average of the tropopause parameters devoid of short-term perturbations like tides and high frequency gravity waves. Below 20°N, the CPT is colder and higher but this relation disappears in subtropics. The effect of tides and high frequency gravity waves on the tropopause temperatures are briefly outlined. The diurnal variability in CPT over Gadanki obtained from INSAT-3D and radiosonde are compared. It is shown that INSAT-3D can be effectively utilized to delineate the tropical tropopause characteristics.

Keywords: Radiosonde measurement, sub-daily variations, tropopause temperature, temporal and spatial resolution.

THE tropical tropopause, which is the interface between the convectively well-mixed troposphere and the stable stratosphere, has attained scientific interest because of its important role in climate variability. Over the tropics, the tropopause is defined based on thermal structure, convection, radiation and chemistry. Based on thermal structure, it is defined as cold point tropopause¹ and lapse rate tropopause. Based on convection, it is defined as convective tropopause. Over the mid-latitudes, the tropopause is defined based on the stability criterion which is quantified by potential vorticity. The World Meteorological Organization (WMO) defined the tropopause based on the lapse rate of temperature obtained over any given location. Lapse rate tropopause is the widely used definition in models for weather forecasting purposes.

The tropopause in the tropics is not a sharp interface but it extends over a few kilometres, defining it to be a layer called tropical tropopause layer (TTL)^{2,3}. The boundaries of the TTL are decided by radiative, convective and thermo-dynamic processes⁴. The TTL extends from the level of the main convective outflow to the cold point tropopause⁵. It is across this layer that the exchange of minor constituents like water vapour, ozone, etc. occurs between the troposphere and the stratosphere⁶. The temperature around the tropopause is very low and is crucial in determining the amount of water vapour being transported into the stratosphere^{7,8}. The long term changes observed in the tropopause temperature (altitude) are considered to be a sensitive indicator of climate change⁹. The variability of the tropopause in synoptic, monthly, seasonal and multi-decadal scales was studied by using radiosonde data obtained from different meteorological stations covering mainly the central western Pacific region¹⁰.

Many studies were carried out in understanding the variability of the tropopause on day to day, monthly, seasonal, annual, inter-annual and multi-decadal time-scales¹¹⁻¹⁵. The changes in the tropopause properties due to many processes (large-scale circulation, small-scale waves and convective influences) play a vital role in the transport of minor species between the troposphere and stratosphere^{2,13}. Several studies have reported the seasonal, monthly and day to day variability of the tropical tropopause over the Indian region^{16,17}. The studies on the variability of the tropopause in relation to convection at sub-daily scales over the land region are very few¹⁸⁻²¹.

However, most of the above-mentioned studies were performed using the conventional radiosondes, which are limited to only a few stations over the Indian region. As a novel and promising tool for observing the tropical tropopause characteristics, here we introduce data obtained from INSAT-3D satellite located in the geostationary orbit. The advantage of the INSAT-3D sounder is its ability to provide hourly measurements of temperature over the entire Indian land mass and every 6 h over the adjoining ocean. In addition to its crucial role in the numerical

*For correspondence. (e-mail: vratnam@narl.gov.in)

Table 1. INSAT-3D sounder channel characteristics (source: Space Applications Centre, Ahmedabad)

Detector	Channel No.	Wavelength (μm)	Principal absorbing gas	Purpose
Longwave	1	14.67	CO ₂	Stratosphere temperature
	2	14.32	CO ₂	Tropopause temperature
	3	14.04	CO ₂	Upper level temperature
	4	13.64	CO ₂	Mid level temperature
	5	13.32	CO ₂	Low level temperature
	6	12.62	H ₂ O	Total precipitable water
	7	11.99	H ₂ O	Surface temperature, moisture
Mid wave	8	11.04	Atmospheric window	Surface temperature
	9	9.72	O ₃	Total ozone
	10	7.44	H ₂ O	Low level moisture
	11	7.03	H ₂ O	Mid level Moisture
	12	6.53	H ₂ O	Upper level moisture
Short wave	13	4.58	N ₂ O	Low level temperature
	14	4.53	N ₂ O	Mid level temperature
	15	4.46	CO ₂	Upper level temperature
	16	4.13	CO ₂	Boundary level temperature
	17	3.98	Atmospheric window	Surface temperature
	18	3.76	Atmospheric window	Surface temperature, moisture
Visible	19	0.695		Cloud detection

weather prediction over India, measurements from the INSAT-3D sounder are useful in understanding the sub-daily scale variability of the tropical tropopause. Details regarding the validation of INSAT-3D data with conventional radiosondes can be found in Venkat Ratnam *et al.*²². In our earlier study on the comparison between INSAT-3D and other datasets, INSAT-3D temperature data showed a consistent warm bias ($\sim 2\text{--}3$ K) in the upper troposphere and lower stratosphere (UTLS) region. The suitability of INSAT-3D data for tropopause study is checked by comparing with radiosonde observations carried out at Gadanki during 2014–2015. Appropriate correction for temperature bias is implemented in the INSAT-3D-derived temperature profile for the tropopause studies.

Data

INSAT-3D

INSAT-3D is an advanced meteorological satellite of India launched from Kourou, French Guiana by Ariane-5 VA-214. It is positioned at 82°E over the equator in a geostationary transfer orbit at an altitude of 35,786 km. The atmospheric sounder with 19 channels (18 in IR + 1 in VIS) in the satellite provides profiles of temperature (T), water vapour (WV) and integrated ozone for every hour over the entire land mass of India and every six hours over the adjoining oceanic regions. The sounder provides data at 40 pressure levels starting from 1000 to 0.1 hPa (i.e. 1000, 950, 920, 850, 750, 700, 670, 620, 570, 500, 475, 430, 400, 350, 300, 250, 200, 150, 135,

115, 100, 85, 70, 60, 50, 30, 25, 20, 15, 10, 7, 5, 4, 3, 2, 1.5, 1, 0.5, 0.2, 0.1 hPa) with a spatial resolution of $0.1^\circ \times 0.1^\circ$ in latitude and longitude. The radiance obtained at different absorption bands during the clear sky conditions is used to retrieve the profiles of T, WV and integrated ozone. Table 1 lists the principal absorbing gases of infrared radiation in the atmosphere at different channels with their purpose of retrieval. The weighting functions for the 18 IR channels are shown in the appendix (Figure A1). The retrieval algorithm adopted is mainly based on that of Hayden²³, Ma *et al.*²⁴ and Li *et al.*²⁵. The algorithm for estimation of temperature adopted by INSAT-3D is the same as that adopted for high-resolution infrared radiation sounder (HIRS) and geostationary operational environmental satellite (GOES). The adopted algorithm by Ackerman *et al.*²⁶ forms the basis for cloud masking feature in the INSAT-3D sounder. The retrieval of temperature and moisture from the INSAT-3D sounder is based on the physical retrieval algorithm over cloud-free regions²⁷. During clear sky conditions, the maximum brightness temperature (BT) in the thermal channel is generated to get a rough idea about the surface temperature. Based on this reference background temperature, the threshold for a particular location is determined to discriminate the cloud. Before determining the pixel to be cloudy, clear, partially cloudy or partially clear, several tests such as BT threshold test, difference test1 (BT11-BT3.7), spatial variability test, spatial uniformity and final threshold test are applied. The hourly temperature data obtained from INSAT-3D during 2014 and 2015 are used in the present study.

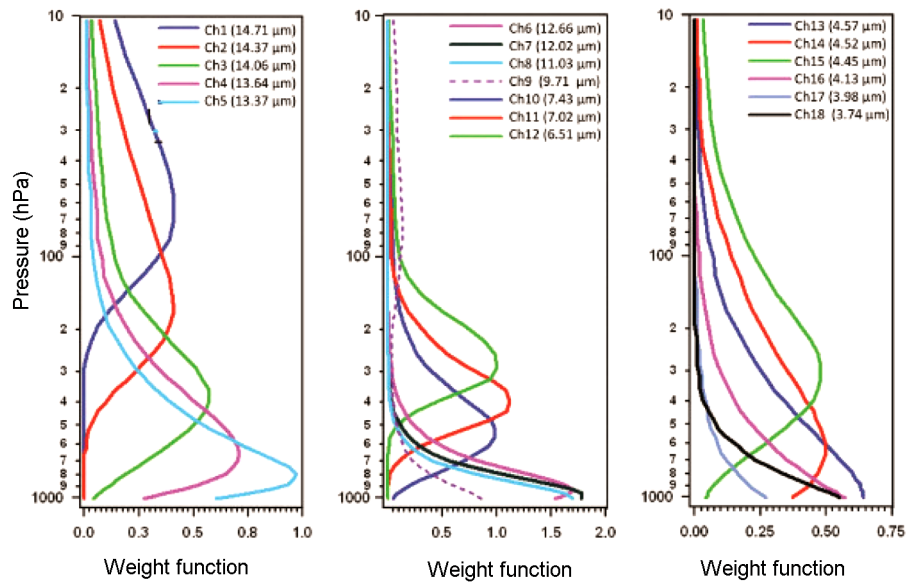


Figure A1. Weighting function representation for 18 channels of INSAT-3D sounder over the Indian region in July. (Source: Space Applications Centre, Ahmedabad, 2015).

GPS radiosondes

In the present study, we utilized temperature data obtained from the high-resolution radiosondes (Meisei RS-11G) launched for every 3 h (02:30, 05:30, 08:30, 11:30, 14:30, 17:30, 20:30 and 23:30 IST) for three consecutive days each month over Gadanki, between December 2010 and March 2014, during a special campaign known as tropical tropopause dynamics (TTD)²⁸. In addition to the TTD campaign data, radiosondes launched over Gadanki around 12 UTC, i.e. 17:30 IST during the years 2014 and 2015 were also used in this study. The temperature was measured using a thermistor of the radiosonde, which was flown into the atmosphere from the surface to ~32–35 km. The basic data were obtained at a vertical resolution of 5–6 m (1 sec interval) with an accuracy of 0.5 K (ref. 28).

Method of estimation of tropopause parameters

The temperature profiles of radiosonde were gridded corresponding to the pressure levels of INSAT-3D before estimating the tropopause parameters. The INSAT-3D temperature profiles corrected with the monthly mean temperature bias (T-bias) were used for deriving tropopause parameters. The T-bias is obtained by the difference between the radiosonde-measured temperature and INSAT-3D derived temperature, as shown in eq. (1).

$$T\text{-bias} = T_{(\text{radiosonde})} - T_{(\text{INSAT-3D})}. \quad (1)$$

The minimum value in the temperature profile was considered to be the cold point tropopause temperature (CPT)

and the pressure level corresponding to CPT as the cold point tropopause pressure (CPH). Whereas, the convective tropopause level was obtained as the level of potential temperature lapse rate was minimum. The temperature corresponding to this level is defined as convective outflow level (COH). The temperature and pressure corresponding to this level are convective tropopause temperature (COT) and convective outflow level pressure (COH pressure). The TTL thickness is defined as the difference between COH and CPT pressure.

Comparison of INSAT-3D and radiosonde-derived temperature in the troposphere

The INSAT-3D-derived temperature in the troposphere and lower stratosphere is compared with collocated GPS radiosonde observations of temperature over Gadanki. Figure 1a shows the mean temperature in the troposphere and lower stratosphere derived from INSAT-3D and radiosonde observations over Gadanki at 12 UTC during the period 2014–2015. The difference in temperature profile between the two is estimated each day. Figure 1b shows the mean of temperature bias (T-bias) with its standard deviation obtained during the same period. The number of collocated profiles used is also superimposed with the top right axis. It is clear from Figure 1a that the temperature obtained from INSAT-3D showed excellent match with that obtained from the radiosondes, though a difference of ~1 and ~0.5 K is noticed between the radiosonde and INSAT-3D in the lower and mid-troposphere respectively (Figure 1b). Negative and positive values of T-bias represent warm and cold biases respectively. There always exists a warm bias in the upper troposphere

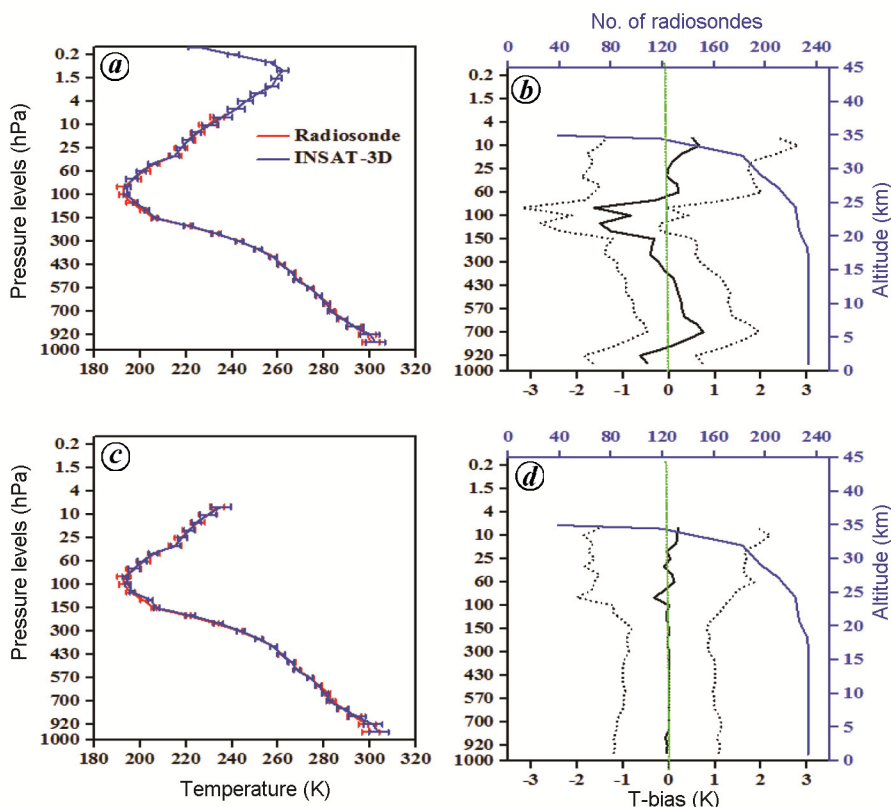


Figure 1. *a*, Mean temperature profiles along with standard deviations observed using INSAT-3D (blue) and Gadanki GPS radiosonde (red) at 12 UTC averaged for the years 2014 and 2015. *b*, Mean and standard deviation of temperature bias (T-bias) obtained during the same period. The number of profiles used is also superimposed with the top right axis. *(c and d)*, Same as *(a)* and *(b)*, but using bias-corrected INSAT-3D temperature profiles.

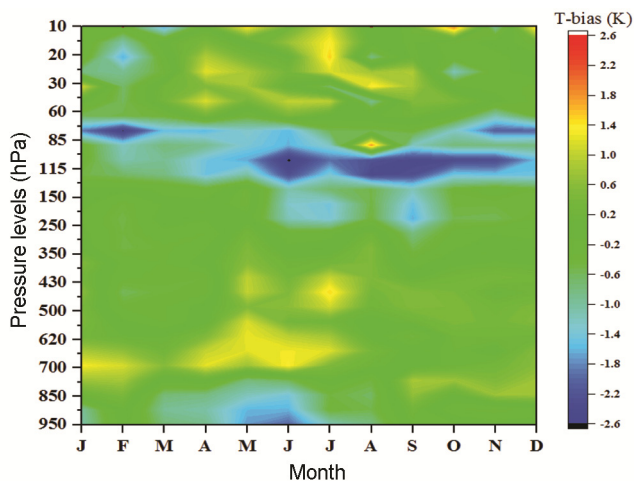


Figure A2. Monthly mean of the temperature bias profile (T-bias) from January to December obtained from INSAT-3D and radiosondes launched around 12 UTC over Gadanki during 2014 and 2015.

(150–70 hPa) with a mean bias of 1–2 K and standard deviation of 2–3 K around 100 hPa in INSAT-3D observations compared with the radiosonde measurements. These observations were in accordance with those of

Singh *et al.*²⁹, wherein they found a warm bias in the region (135–100 hPa) with a mean bias of +1 K around 115 hPa during validation of INSAT-3D sounder data over a larger domain (52°–100°E and 14°S–40°N). The bias was estimated at each pressure level every month and the monthly mean bias value was removed from the INSAT-3D temperature profile. The mean altitudinal T-bias profile for each month is given in the Appendix (Figure A2). Figure 1 *c* shows the mean and standard deviation in temperature obtained from the bias-corrected temperature profiles of INSAT-3D and radiosonde temperature profiles. Figure 1 *d* shows the mean and standard deviation of temperature bias obtained between the radiosonde and bias-corrected INSAT-3D profiles during the same period. It is clear from Figure 1 *d* that the difference in temperature is nullified when the bias-corrected temperature profiles of INSAT-3D are used for comparison, though noticeable standard deviation still exists perhaps due to day-to-day variability of temperature.

Altitude profile of monthly mean T-bias obtained from this comparison was used to correct the temperature profile of INSAT-3D for all profiles obtained during 2014 and 2015 over the Indian region. The tropopause parameters such as CPT and CPH, COT and COH and TTL

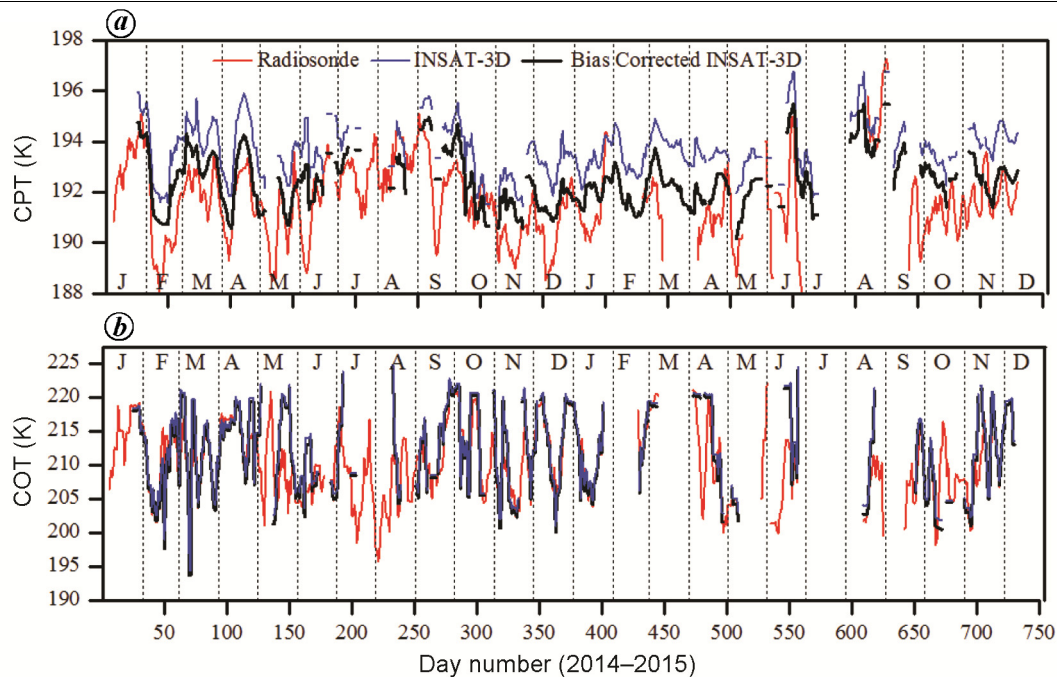


Figure 2. *a*, Time series of cold point tropopause (CPT) temperature at 12 UTC obtained from INSAT-3D profiles (blue), bias-corrected INSAT-3D profiles (black) and radiosondes (red) over Gadanki during the period January 2014 to December 2015. *b*, Same as (*a*), but for COT (convective tropopause temperature).

thickness were estimated from the actual and monthly mean T-bias-corrected temperature profiles of INSAT-3D, and compared with that derived from radiosonde observations. Figure 2 shows the CPT and COT derived from actual and bias-corrected temperature profiles of INSAT-3D around 12 UTC over Gadanki during 2014 and 2015 along with those derived from collocated radiosonde observations. The distribution of difference in tropopause temperatures (CPT and COT) obtained from the actual INSAT-3D temperature and bias-corrected INSAT-3D profile and the radiosonde-obtained tropopause temperatures during the same period is shown in the Appendix (Figure A3). INSAT-3D mostly shows a warm bias of ~ 2 and 3 K in CPT and COT respectively, when compared with the radiosonde estimated CPT and COT (Figure A3 *a*). The tropopause temperatures (CPT and COT) estimated from the bias-corrected INSAT-3D temperature profiles were also superimposed along with the tropopause temperatures obtained from the actual INSAT-3D temperature and radiosonde temperature profiles (Figure 2 *a* and *b*). The difference in temperature was mostly between -1 and -4 K for both CPT and COT (Figure A3 *a* and *b*). However the difference in temperature showed a decrease (peaks around 0 and -1 K for both CPT and COT) when bias-corrected profiles were used (Figure A3 *c* and *d*). This provides an insight of using INSAT-3D sounder data for obtaining tropopause characteristics with known consistent biases instead of the radiosonde, as observations using the latter are sparse and available only two times a day (00 and 12 UTC) at the

best, unlike INSAT-3D where observations are available at hourly intervals covering the complete Indian region. The tropopause parameters obtained from INSAT-3D presented in the subsequent sections were derived from the monthly mean bias-corrected temperature profiles of the satellite.

TTL characteristics over the Indian region

Though the INSAT-3D sounder does not provide high vertical resolution temperature measurements unlike radiosondes that resolve small-scale fluctuations occurring in the tropopause region due to gravity waves and other processes, these observations are sufficient to delineate the broad features. The hourly temperature data obtained from the INSAT-3D sounder over the Indian region during 2014 and 2015 were corrected with the monthly mean T-bias and then used for estimating the tropopause parameters. The daily mean profiles obtained from the hourly data were used to estimate the tropopause parameters and thus obtain seasonal mean tropopause parameters (CPT, CPH, COT, COH and TTL). This analysis provides the actual picture of tropopause parameters during different seasons as the short-period waves like high-frequency gravity waves and tides will be mostly removed while averaging the tropopause parameters hourly. The result of such analysis provides true seasonal means unlike that reported by other satellite measurements, as the overpass of those satellites over a given

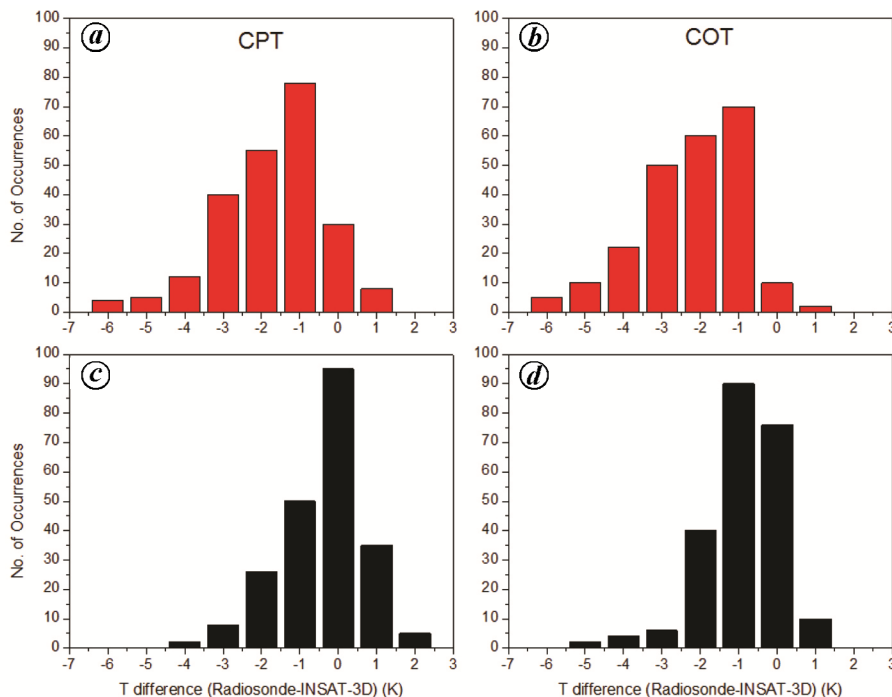


Figure A3. Histograms showing the distribution of the difference in cold point tropopause temperature (CPT) between radiosonde and INSAT-3D. (b) Same as (a) but for COT. (c and d) Same as (a) and (b) but for the difference obtained in CPT and COT from the bias corrected INSAT-3D and radiosonde temperature profiles.

location does not cover complete diurnal cycle and thus contribution of waves and oscillations will remain. Tidal signatures observed in the tropopause parameters will be discussed later in the text.

Figures 3 and 4 show the spatial variation of CPT and CPH during different seasons obtained from INSAT-3D during 2014 and 2015. While comparing INSAT-3D with other satellites (MLS, AIRS), we have found that there exists large bias in the INSAT-3D measurements above 30°N (ref. 22) and thus, we restrict our analysis up to 30°N only for any meaningful discussion. From Figure 3, it is clear that the CPT is colder and warmer in equatorial region and sub-tropics respectively, during all the seasons. Below 20°N , CPT is colder during pre-monsoon (MAM) and winter (DJF), while it is relatively warmer during the monsoon (JJA) and post-monsoon (SON) seasons. Whereas CPH obtained from INSAT-3D is higher (lower the altitude) during monsoon and post-monsoon and lower (higher the altitude) during winter and pre-monsoon seasons (Figure 4). These results are in accordance with those of Krishna Murthy *et al.*³⁰ over the Indian region using India Meteorological Department (IMD) radiosonde at 11 stations spread over 8.5° – 28.6°N , and by Gage and Reid³¹ over other tropical locations. The CPT and altitude are exactly in opposite phase in the equatorial region. It is interesting to note from Figures 3 and 4 that the presence of exactly opposite phase during all the seasons between CPT and CPH progressively dis-

appears beyond 20°N and becomes insignificant in the subtropics, similar to that observed by Sunilkumar *et al.*¹⁷ and Venkat Ratnam *et al.*³². The disappearance of the opposite phase between CPT and altitude in the subtropics over the Indian region may be due to the presence of monsoon circulation, as reported by Randel *et al.*³³. At higher latitudes ($>20^{\circ}\text{N}$), CPT is coldest and warmest during monsoon and winter seasons respectively. The enhancement of anti-cyclonic circulation in the upper troposphere during the Asian summer monsoon might be responsible for the observed tropopause variation³⁴. The reduction in longwave radiation absorption by ozone in the lower stratosphere due to the presence of high-level clouds during active convection is also a factor for the observed variation of the tropopause temperature³⁵.

Figures 5 and 6 show the seasonal mean of COT and COH obtained over each latitude–longitude grid of INSAT-3D observations respectively. Above 10° North latitude, the convective tropopause is cooler and higher during monsoon indicating the role of intense convection over the Indian region pertaining to monsoon circulation.

The seasonal mean of TTL thickness is inferred from the mean of the difference between CPH and COH (Figure 7). Low pressure difference between CPH and COH during monsoon within the tropics indicates smaller TTL thickness. This gives an insight about the possibility of vertical transport into lower stratosphere due to active convection present over this region. The narrowing of the

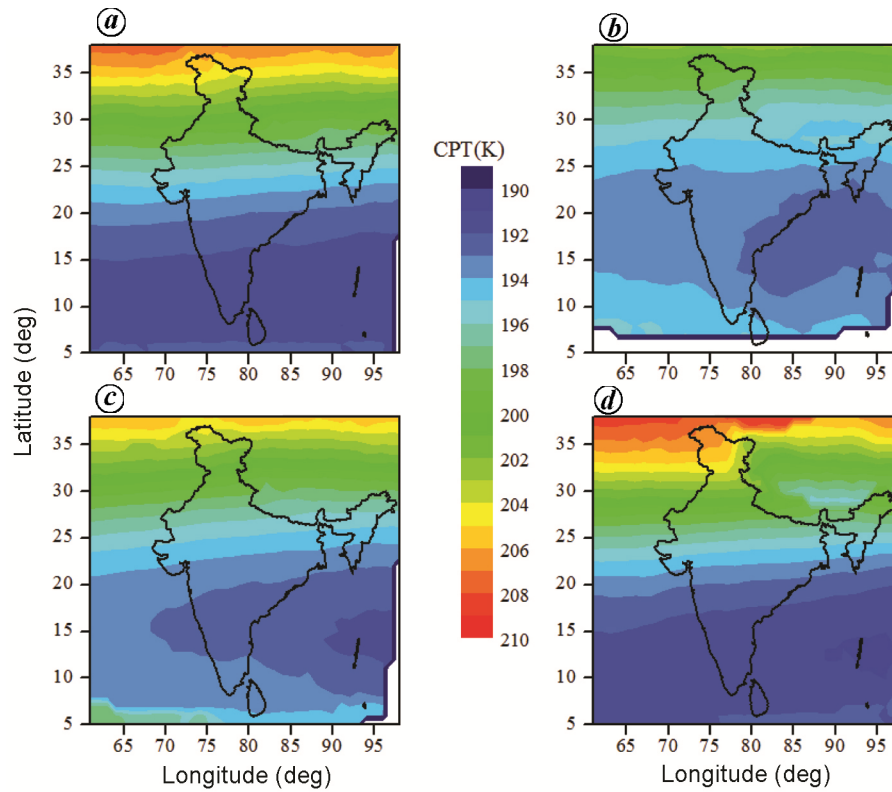


Figure 3. Spatial variation of cold point tropopause temperature (CPT) during (a) pre-monsoon, (b) monsoon, (c) post-monsoon and (d) winter over the Indian region obtained from the bias-corrected INSAT-3D profiles (January 2014–December 2015).

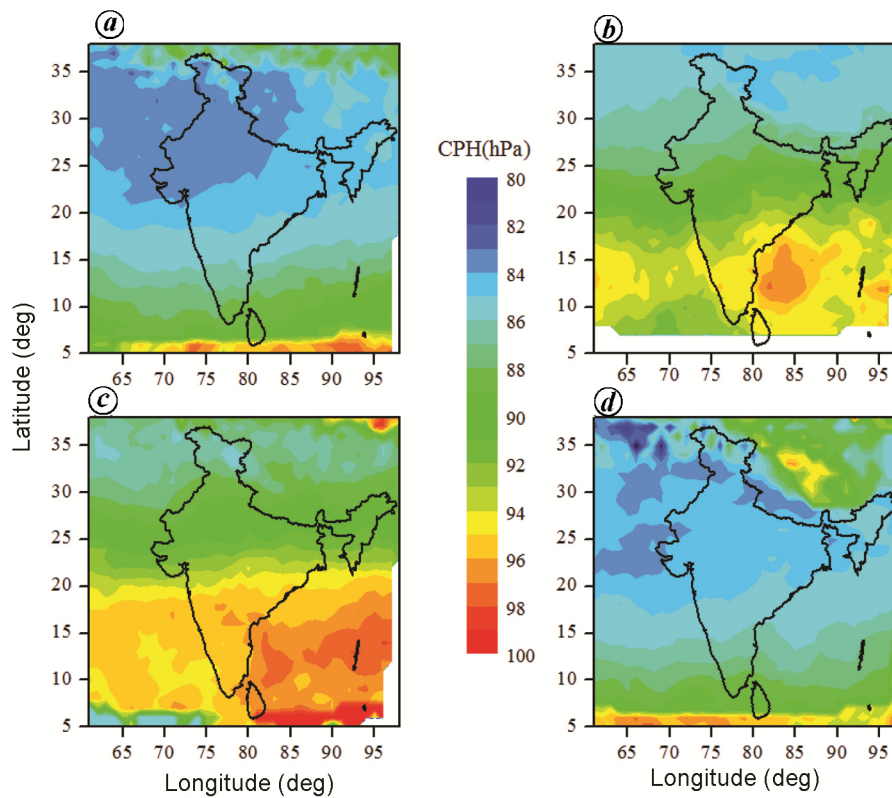


Figure 4. Same as Figure 3, but for cold point tropopause pressure (hPa).

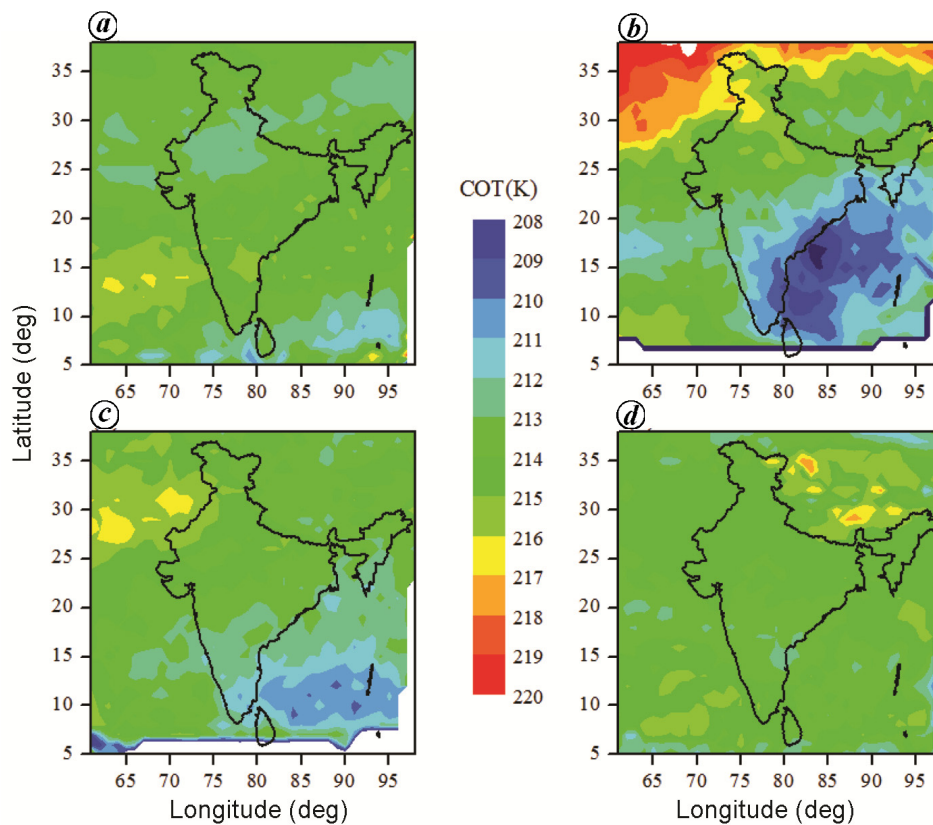


Figure 5. Same as Figure 3, but for convective tropopause temperatures (K).

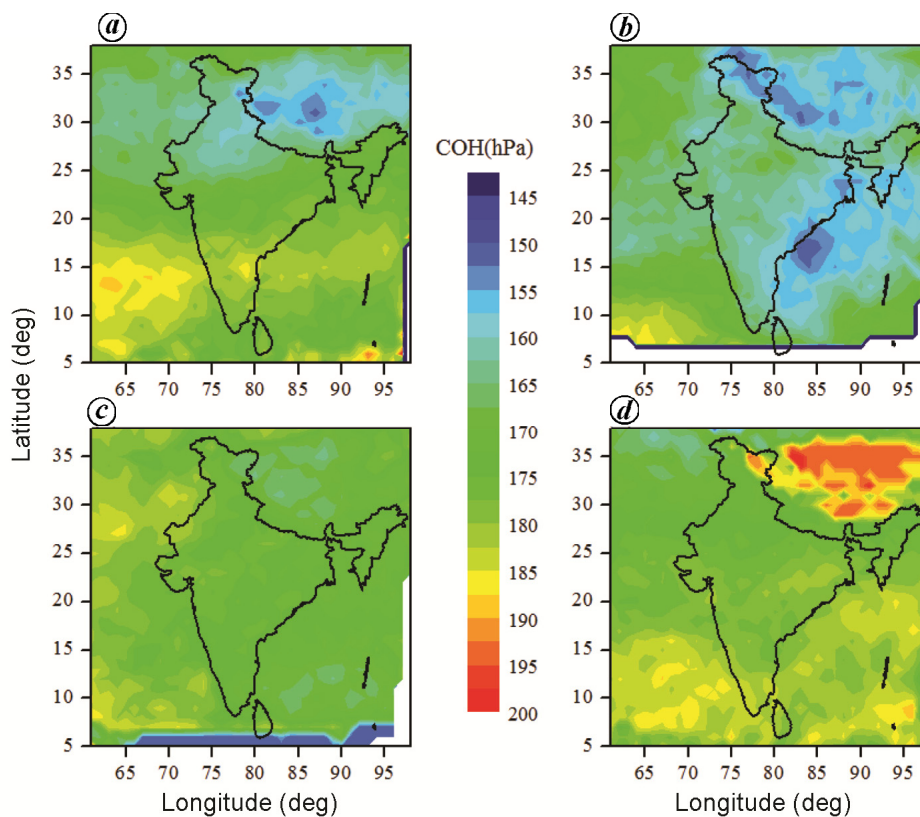


Figure 6. Same as Figure 3, but for convective tropopause pressure (hPa).

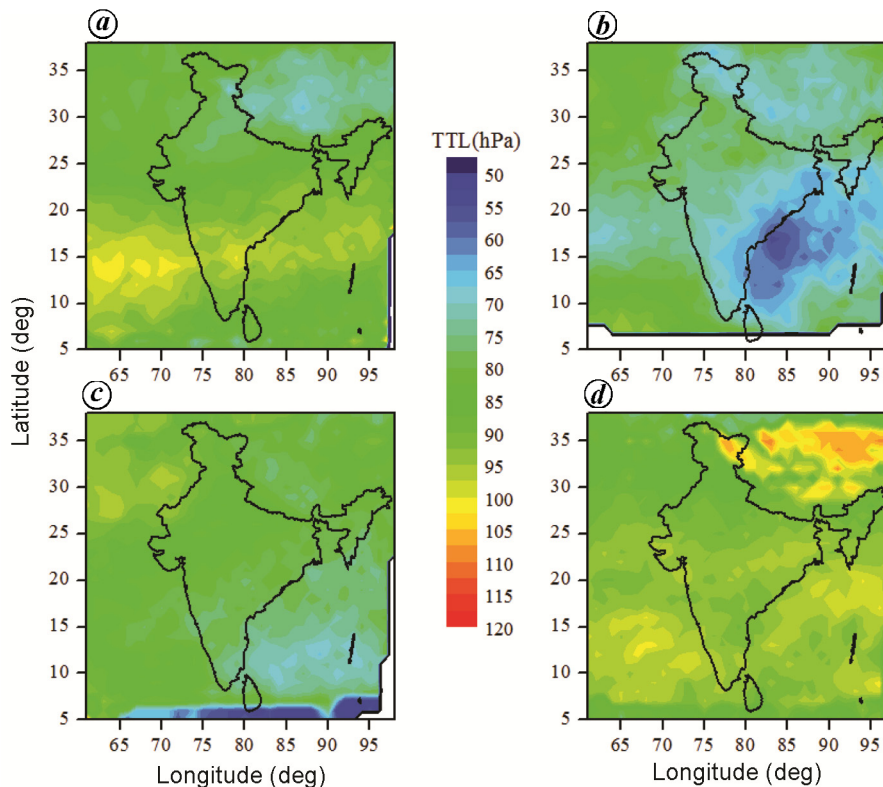


Figure 7. Same as Figure 3, but for the tropical tropopause layer thickness (hPa).

TTL inferred during the monsoon season is attributed to the descending CPH and ascending COH²¹. The TTL thickness is narrower over the Bay of Bengal than the Arabian Sea, indicating the convection to be deep and shallow respectively^{36,37}. There is large scope for Stratospheric and Tropospheric Exchange (STE) processes over the head Bay of Bengal as TTL thickness is narrower during monsoon season. The increase in TTL thickness below 20°N is clearly evident during the winter and pre-monsoon seasons, which is due to the low CPH (high altitude) and high COH (low altitude), as observed in Figures 4 and 6.

Figure 8 shows the zonal mean latitude variation of tropopause parameters (CPT, CPH, COT and COH) between 5°N and 30°N for different seasons (pre-monsoon, monsoon, post-monsoon and winter). This is derived from the hourly data of INSAT-3D during the period January 2014–December 2015. As discussed earlier CPT is colder and lower (high pressure) within the equatorial latitudes (up to 10°–15°N). It is also found that the CPH altitude (CPH pressure) is lower (higher) over the equatorial region and higher (lower) in the subtropics. Similar features have already been reported by Venkat Ratnam *et al.*³² using GPS RO measurements. Similar type of feature has also been reported over the Indian region by Sunilkumar *et al.*¹⁷ using COSMIC RO data and radiosonde observations, wherein they observed a dip in the cold point tropopause altitude over the equatorial

region and its increase gradually towards north and south. Further evidence of U-shaped structure for cold point tropopause altitude (i.e. lower in the equatorial latitudes and higher in the subtropics) is observed from INSAT-3D observations over the Indian region. This U-shaped structure is more pronounced during winter and pre-monsoon followed by monsoon and post-monsoon seasons. However, the CPT temperature is warmer and CPH pressure is lower beyond 15°N (Figures 3 and 4). This inverse relation gradually decreases towards latitudes north of 20°N. The CPT temperature increases gradually from 15° up to 25°N, after which there is a sharp increase. However, CPH–pressure (CPH altitude) shows a gradual decrease (increase) up to 25°N during winter, and up to 30°N during rest of the seasons. Within the tropics, the COT temperature is colder during the monsoon season compared to other seasons. The latitudinal variation of COT is very small over the Indian region, though large variation in COH is observed. Thus, INSAT-3D data can be effectively used to study the tropopause characteristics.

Tidal signatures in the tropopause temperature

The seasonal mean of the tropopause parameters (CPT, CPH, COT, COH and TTL) was obtained from the hourly INSAT-3D sounder data. The short-period oscillations were averaged out in the seasonal mean of the tropopause

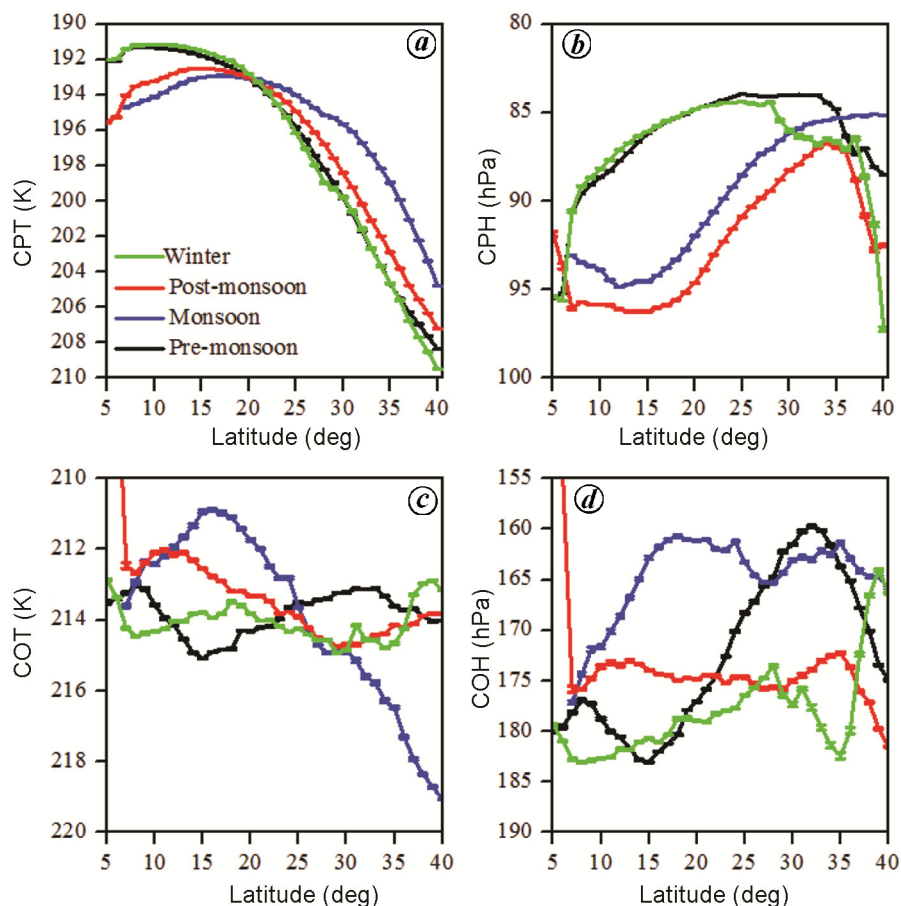


Figure 8. *a*, Zonal mean (60° – 100° E) latitudinal variation of CPT obtained from INSAT-3D for the years 2014 and 2015 observed during pre-monsoon (black), monsoon (blue), post-monsoon (red) and winter (green). Vertical bars show the standard error obtained for the corresponding seasons. *b*, Same as (*a*), but for CPH. *c*, same as (*a*), but for COT (K). (*d*), Same as (*a*), but for COH (hPa).

parameters, as they have been obtained from the hourly INSAT-3D sounder data. In order to know the significance of diurnal variation, temperature profiles obtained from INSAT-3D and radiosonde during the TTD campaign conducted between January 2014 and March 2014 were used. The INSAT-3D temperature profiles for each month were corrected with the monthly mean T-bias profile before being used. As mentioned earlier, we have conducted three hourly radiosonde launches as a part of TTD campaigns during 27–30 January 2014, 24–27 February 2014 and 25–28 March 2014. Figure 9*a*, *d* and *g* shows the diurnal mean from three-days temperature profiles of these three campaigns respectively, obtained from INSAT-3D and radiosonde. A good match between the INSAT-3D and radiosonde profiles can be noticed. The short-period waves and tides modulate the tropopause parameters. The perturbation in temperature using radiosonde observations at 00 and 12 UTC was estimated by subtracting the diurnal mean (obtained from the three hourly temperature profiles of radiosondes launched continuously for three days in each month) and the mean

temperature profiles obtained at 00 and 12 UTC respectively from three days (Figure 9*b*, *e* and *h*). Figure 9*c*, *f* and *i* shows the perturbation in temperature at 00 and 12 UTC using INSAT-3D observations. However, the diurnal mean in this case was obtained from the hourly temperature profiles obtained from INSAT-3D after bias correction. Contrasting difference in temperature between 00 and 12 UTC can be noticed in both radiosonde and INSAT-3D observations, indicating strong diurnal variation in temperature, particularly due to tides. A difference of 4 K is noticed between 00 and 12 UTC up to 850 hPa, whereas the difference is 1–2 K near the vicinity of 100 hPa. Several reports have suggested that the tides which are considered to be the oscillations due to solar heating of water vapour in the troposphere and ozone in the stratosphere are potent enough in modulating the tropopause temperature^{38,39}. The magnitude of temperature perturbation around 12 and 00 UTC in the stratosphere is stronger as seen in Figure 9*c* and *f*, indicating the progressive growth of tidal amplitude at higher altitudes. The increase in magnitude of temperature perturbation in the

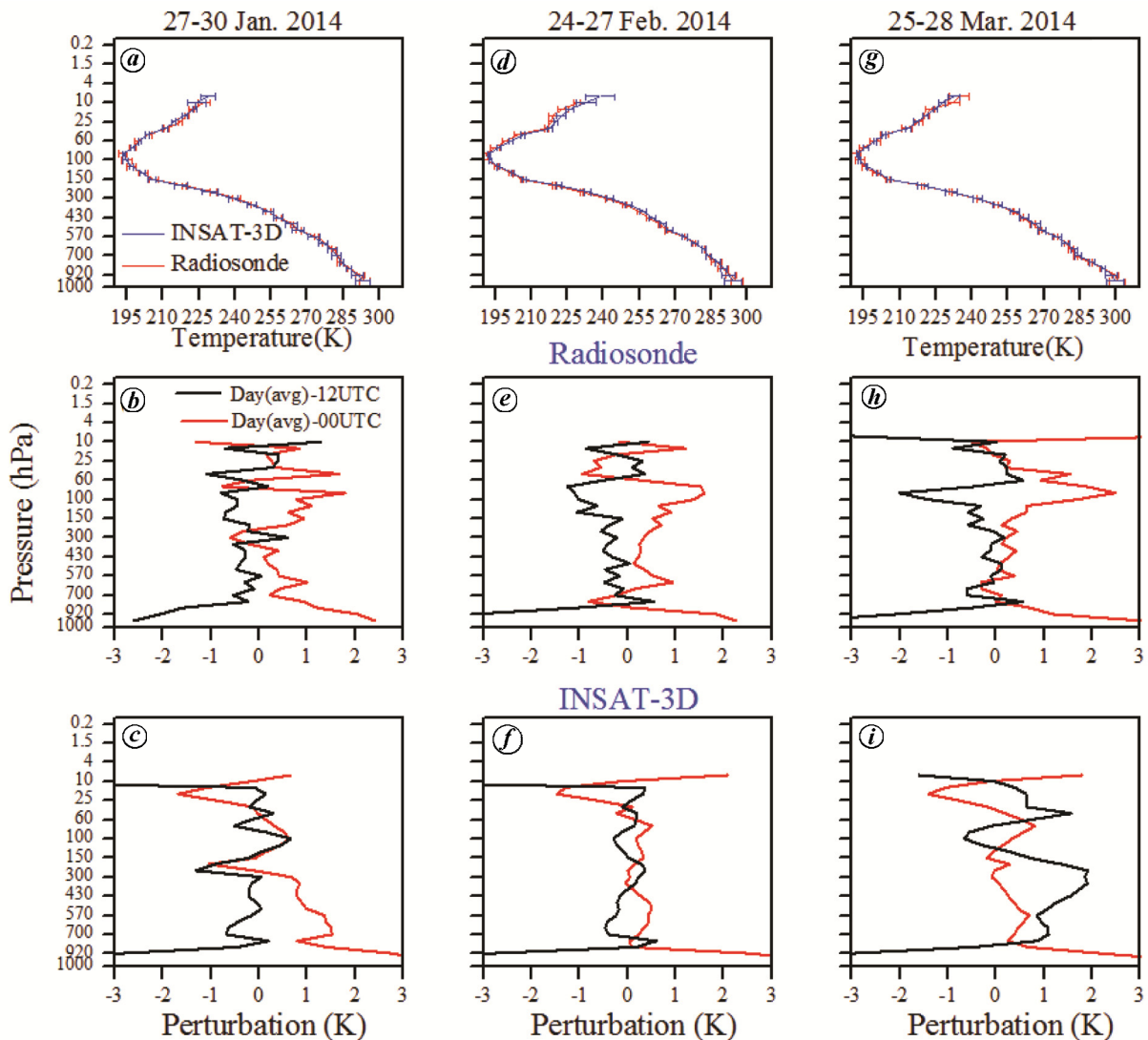


Figure 9. *a*, Mean profiles of temperature obtained from Gadanki radiosonde (red) and INSAT-3D (blue) during 27–30 January 2014 as a part of tropical tropopause dynamics campaigns. Horizontal bars show standard deviations. *b*, Perturbation in temperature observed at 00 and 12 UTC obtained from the three-hourly observations of the radiosonde during the same period. *c*, Same as (*b*), perturbation obtained from the hourly INSAT-3D observations during the same period. (*d*–*f*), Same as (*a*–*c*), but obtained during 24–27 February 2014. (*g*–*i*). Same as (*a*–*c*), but obtained during 25–28 March 2014.

stratosphere is not seen due to the ceiling of the radiosonde observations associated with balloon bursts.

In order to observe the dominant periods, an empirical mode decomposition (EMD) technique was performed to the hourly tropopause temperatures (CPT and COT) estimated from INSAT-3D sounder data. This method decomposes the oscillations into characteristic components called intrinsic mode function (IMF). The methodology involved in extracting the IMF by EMD technique has been clearly explained by Kishore *et al.*⁴⁰ In this technique, higher frequencies were obtained in the first IMF component followed by relatively lower average frequencies in the subsequent IMF components. The local characteristic timescales of the data themselves were used in determining the number of modes and frequency of each

mode^{41,42}. The Lomb–Scargle periodogram was calculated for various IMFs using the hourly tropopause temperatures (CPT and COT) obtained from INSAT-3D over Gadanki (Figure 10). The bias-corrected temperature profiles were used for determining the CPT and COT. In Figure 10, the 90% confidence level is shown by a horizontal dotted line. Though spectral analysis was performed to the hourly data obtained over Gadanki between January 2014 and December 2015, the periods which were dominant for less than eight-days are only shown in Figure 10. A strong peak at a period of 24 and 12 h is clearly visible in the original time series of CPT (Figure 10 *a*) and COT (Figure 10 *b*). The 3–4 h period is clearly observed in CPT but not in the COT in IMF1 (Figure 10 *c* and *d* respectively). Whereas CPT and COT show an

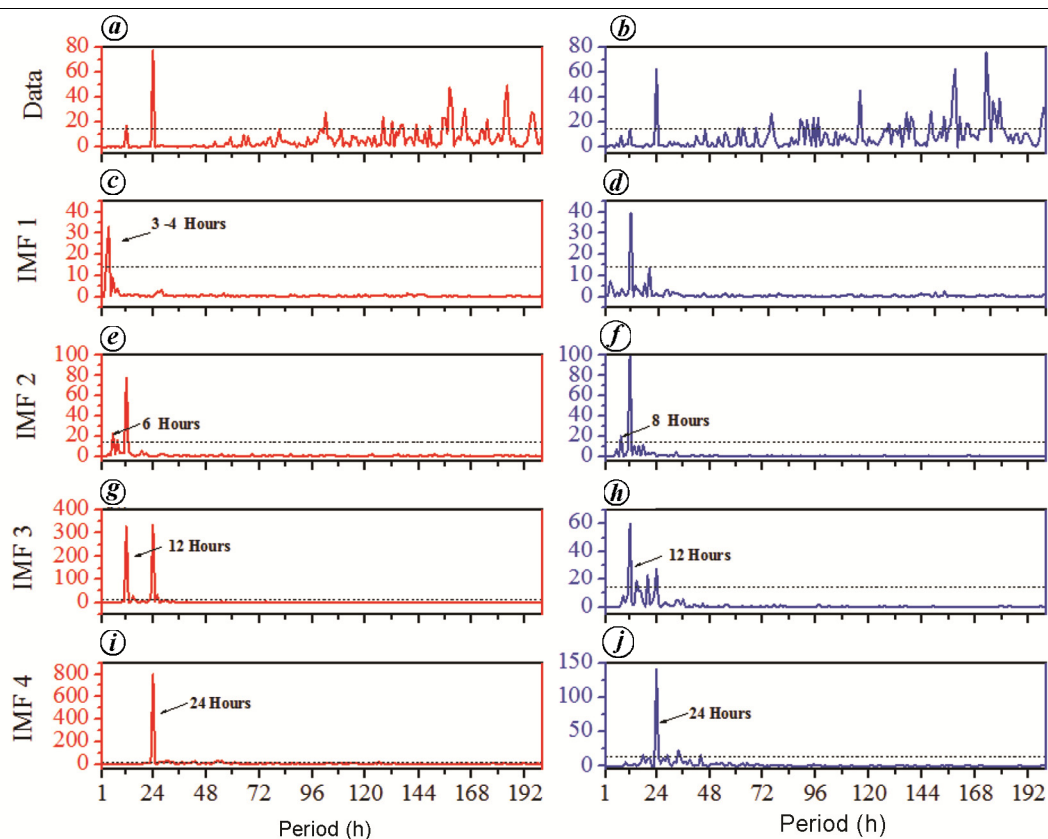


Figure 10. Lomb-Scargle periodograms obtained from various intrinsic mode functions for (a, c, e, g, i) CPT and (b, d, f, h, j) COT obtained from bias-corrected INSAT-3D temperature profiles during 2014–2015. The dotted line shows 90% confidence level.

period of 6 and 8 h respectively, in IMF 2 (Figure 10e and f respectively). However, the semi-diurnal and diurnal oscillations are clearly visible in IMF3 and IMF4 in both the CPT and COT. Thus, tides (diurnal and semi-diurnal) play a significant role in modulating the tropopause parameters.

Sub-daily scale variability of CPT during different seasons

To study the sub-daily scale variability in the tropopause parameters, we considered the temperatures of the CPT. Since we did not have an overlap period of more than three months between INSAT-3D and TTD campaigns, we considered complete TTD campaign data obtained over Gadanki between December 2010 and March 2014 to show qualitatively the sub-daily scale variability. Figure 11 shows the comparison of diurnal variability in CPT obtained over Gadanki from radiosonde during the TTD campaign for different seasons with the diurnal variability of CPT obtained from INSAT-3D for 2014 and 2015. The bias-corrected INSAT-3D temperature profiles were to determine CPT temperatures.

The mean CPT measured from INSAT-3D during different seasons match well with that obtained from radio-

sonde. Low and high CPT were observed during winter and monsoon respectively, using both techniques. The large variability in CPT obtained from INSAT-3D during all seasons (error bars in Figure 11a–d) is due to the coarse altitude resolution in INSAT-3D observations. The sub-daily scale variability in CPT is clearly observed from INSAT-3D during all seasons. The CPT obtained from INSAT-3D over Gadanki shows almost similar pattern as that made by radiosonde over the same location, though the amplitudes of the diurnal cycle are small. During all seasons, CPT increases slowly after sunrise and attains a peak value at around 11:30 and 14:30 IST, and again decreases and reaches a minimum value during midnight and early morning hours (before sunrise). Low CPT corresponds to high CPH. This result matches with that of Suneeth *et al.* who reported warmer CPT during the early afternoon and colder during the late evening⁴³. It is also observed that CPT is warmer prior to the peak occurrence of convection, which is generally in the evening²¹.

Summary and conclusion

The ability of the INSAT-3D sounder data in picking up the tropopause characteristics over the entire Indian

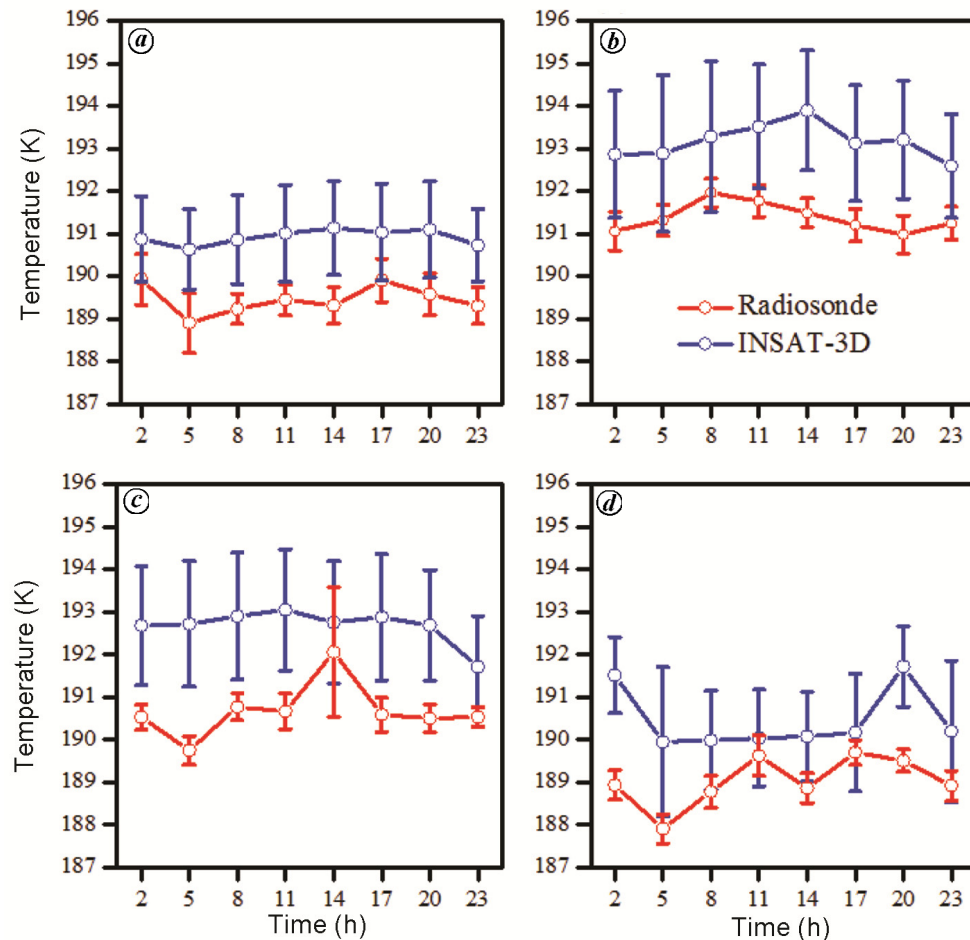


Figure 11. Mean diurnal variation of CPT obtained from radiosonde temperature profiles (red; 2010–2014) and bias-corrected INSAT-3D temperature profiles (blue; 2014–2015) over Gadanki during (a) pre-monsoon, (b) monsoon, (c) post-monsoon and (d) winter season. Vertical bars show the standard deviation.

region is discussed here. The bias in temperature around the UTLS region is estimated by comparing the INSAT-3D sounder data with the well-established conventional *in situ* radiosonde observations made over Gadanki. The monthly mean T-bias is used for correcting INSAT-3D temperature before it is utilized for estimating the tropopause parameters. The tropopause characteristics (CPT, CPH, COT, COH and TTL) obtained from INSAT-3D during different seasons over the Indian region is discussed. The main findings are summarized as follows:

(1) There exists a consistent warm bias of 2–3 K in the INSAT-3D observations in the UTLS region when compared with the collocated radiosonde observations. After correcting this bias, it is shown that the data can be effectively used to estimate tropopause parameters.

(2) As the tropopause parameters from INSAT-3D are available for every hour over the complete Indian region, the mean variation in these parameters provides the true seasonal mean unlike that obtained by other satellite measurements, as contribution from the tides and waves will be removed.

(3) The CPT temperature and altitude of CPT are in opposite phase in the equatorial region during all seasons. However, this feature progressively decreases north of 20°N and becomes insignificant in the subtropics. This stronger inverse relationship in the equatorial region may be due to high contribution of stratospheric processes, whereas in the subtropics weakening of this inverse relationship is attributed to the influence of tropospheric active convection associated with the Asian summer monsoon⁴⁴.

(4) Convective tropopause is cooler and higher in the north of 10°N during monsoon, indicating the role of intense convection over the Indian region pertaining to monsoon circulation.

(5) TTL thickness inferred from INSAT-3D is small during the monsoon season, thus providing an insight about the possibility of vertical transport into the lower stratosphere due to the active convection present over this region. Interestingly, TTL thickness is narrow over the Bay of Bengal than the Arabian Sea indicating convection to be deep and shallow respectively. The TTL

thickness increases during the winter and pre-monsoon seasons in the tropics.

(6) Further evidence of U-shaped structure for cold point tropopause altitude (i.e. lower in the equatorial latitudes and higher in the subtropics) is observed from the INSAT-3D observations over the Indian region.

(7) The latitudinal variation of COT is very small over the Indian region, though large variation in the COH is observed.

(8) Variability up to 4 K in the tropopause temperature due to dominant diurnal and semi-diurnal tides is noticed. Dominant 3–4 h period oscillations indicate the role of high-frequency gravity waves in the CPT temperatures, but not in the COT. Thus, tides and waves play a significant role in modulating the tropopause parameters.

(9) The sub-daily scale variability in CPT is clearly observed in the INSAT-3D measurements during all seasons. The CPT obtained from INSAT-3D over Gadanki shows almost similar features as that of the collocated radiosonde observations.

Thus, it is shown that INSAT-3D data can be effectively used to study the tropopause characteristics. Since the observations are available at hourly resolution at every grid of 10 km × 10 km, the data can be effectively utilized for studying the STE processes even at sub-daily scales.

1. Selkirk, H. B., The tropopause cold trap in the Australian monsoon during STEP/AMEX 1987. *J. Geophys. Res. Atmos.*, 1993, **98**, 8591–8610.
2. Randel, W. J. and Jensen, E. J., Physical processes in the tropical tropopause layer and their roles in a changing climate. *Nature Geosci.*, 2013, **6**, 169–176.
3. Fueglistaler, S., Dessler, A. E., Dunkerton, T. J., Folkins, I., Fu, Q., and Mote, P. W., Tropical tropopause layer. *Rev. Geophys.*, 2009, **47**, 1–31.
4. Sunilkumar, S. V., Muhsin, M., Venkat Ratnam, M., Parameswaran, K., Krishna Murthy, B. V. and Emmanuel, M., Boundaries of tropical tropopause layer (TTL): a new perspective based on thermal and stability profiles. *J. Geophys. Res.-Atmos.*, 2017, **122**, 741–754.
5. Gettelman, A. and Forster, P. M., A climatology of the tropical tropopause layer. *J. Meteorol. Soc. Jpn*, 2002, **80**, 911–924.
6. Holton, J. R., Haynes, P. H., McIntyre, M. E., Douglass, A. R., Rood, R. B. and Pfister, L., Stratosphere–troposphere exchange. *Rev. Geophys.*, 1995, **33**, 403–439.
7. Mote, P. W. *et al.*, An atmospheric tape recorder: The imprint of tropical tropopause temperatures on stratospheric water vapor. *J. Geophys. Res.-Atmos.*, 1996, **101**, 3989–4006.
8. Robinson, G. D., The transport of minor atmospheric constituents between troposphere and stratosphere. *Q. J. R. Meteorol. Soc.*, 1980, **106**, 227–253.
9. Santer, B. D. *et al.*, Response to comment on ‘Contributions of anthropogenic and natural forcing to recent tropopause height changes’. *Science*, 2004, **303**, 1771.
10. Seidel, D. J. and Randel, W. J., Variability and trends in the global tropopause estimated from radiosonde data. *J. Geophys. Res.-Atmos.*, 2006, **111**, 1–17.
11. Gage, K. S. and Reid, G. C., Solar variability and the secular variation in the tropical tropopause. *Geophys. Res. Lett.*, 1981, **8**, 187–190.
12. Tsuda, T., Murayama, Y., Wiryosumarto, H., Harijono, S. W. B., and Kato, S., Radiosonde observations of equatorial atmosphere dynamics over Indonesia 2. Characteristics of gravity waves. *J. Geophys. Res.-Atmos.*, 1994, **99**.
13. Reid, G. C. and Gage, K. S., The tropical tropopause over the western Pacific: wave driving, convection, and the annual cycle. *J. Geophys. Res.-Atmos.*, 1996, **101**(D16), 21233–21241.
14. Shimizu, A. and Tsuda, T., Variations in tropical tropopause observed with radiosondes in Indonesia. *Geophys. Res. Lett.*, 2000, **27**, 2541–2544.
15. Ratnam, M. V., Tsuda, T., Mori, S. and Kozu, T., Modulation of tropopause temperature structure revealed by simultaneous radiosonde and CHAMP GPS measurements. *J. Meteorol. Soc. Jpn*, 2006, **84**, 989–1003.
16. Parameswaran, K., Thampi, B. V. and Sunilkumar, S. V., Latitudinal dependence of the seasonal variation of particulate extinction in the UTLS over the Indian longitude sector during volcanically quiescent period based on lidar and SAGE-II observations. *J. Atmos. Sol.-Terres. Phys.*, 2010, **72**, 1024–1035.
17. Sunilkumar, S. V., Babu, A. and Parameswaran, K., Mean structure of the tropical tropopause and its variability over the Indian longitude sector. *Climate Dyn.*, 2013, **40**, 1125–1140.
18. Johnson, R. H., Short-term variations of the tropopause height over the winter MONEX area. *J. Atmos. Sci.*, 1986, **43**(11), 1152–1163.
19. Mehta, S. K. *et al.*, Identification of tropical convective tropopause and its association with cold point tropopause. *J. Geophys. Res.-Atmos.*, 2008, **113**, 2–9.
20. Sherwood, S., Horinouchi, T. and Zeleznik, H., Convective impact on temperatures observed near the tropical tropopause. *J. Atmos. Sci.*, 2003, **60**, 1847–1857.
21. Kumar, A. H., Ratnam, M. V., Sunilkumar, S. V., Parameswaran, K. and Murthy, B. V. K., Role of deep convection on the tropical tropopause characteristics at sub-daily scales over the South India monsoon region. *Atmos. Res.*, 2015, **161–162**, 14–24.
22. Venkat Ratnam, M., Hemanth Kumar, A. and Jayaraman, A., Validation of INSAT-3D sounder data with *in situ* measurements and other similar satellite observations over India. *Atmos. Meas. Tech.*, 2016, **9**, 5735–5745.
23. Hayden, M. C., GOES-VAS temperature–moisture retrieval algorithm. *J. Appl. Meteorol.*, 1988, **27**, 705–733.
24. Ma, X. L., Schmit, T. J. and Smith, W. L., A nonlinear physical retrieval algorithm – its application to the GOES-8/9 sounder. *J. Appl. Meteorol.*, 1999, **38**, 501–513.
25. Li, J., Wolf, W. W., Menzel, W. P., Zhang, W., Huang, H. L. and Achtor, T. H., Global soundings of the atmosphere from ATOVS measurements: The algorithm and validation. *J. Appl. Meteorol.*, 2000, **39**, 1248–1268.
26. Ackerman, S. A., Strabala, K. I., Menzel, W. P., Frey, R. A., Moeller, C. C., and Gumley, L. E., Discriminating clear sky from clouds with MODIS. *J. Geophys. Res. Atmos.*, 1998, **103**, 32141–32157.
27. Li, J., Wolf, W. W., Menzel, W. P., Zhang, W., Huang, H.-L. and Achtor, T. H., Global soundings of the atmosphere from ATOVS measurements: the algorithm and validation. *J. Appl. Meteorol.*, 2000, **39**, 1248–1268.
28. Venkat Ratnam, M. *et al.*, Tropical tropopause dynamics (TTD) campaigns over Indian region: an overview. *J. Atmos. Solar-Terrestrial Phys.*, 2014, **121**, 229–239.
29. Singh, T., Mittal, R. and Shukla, M. V., Validation of INSAT-3D temperature and moisture sounding retrievals using matched radiosonde measurements. *Int. J. Remote Sens.*, 2017, **38**, 3333–3355.
30. Krishna Murthy, B. V., Parameswaran, K. and Rose, K. O., Temporal variations of the tropical tropopause characteristics. *J. Atmos. Sci.*, 1986, **43**(9), 914–922.

31. Gage, K. S. and Reid, G. C., Aeronomy Laboratory National Oceanic and Atmospheric Administration Boulder, Colorado 80303. 1981, **8**, 187–190.
32. Ratnam, M. V., Tsuda, T., Shiotani, M. and Fujiwara, M., New characteristics of the tropical tropopause revealed by CHAMP/GPS measurements. *Sola*, 2005, **1**, 185–188.
33. Randel, W. J., Wu, F. and Gaffen, D. J., Interannual variability of the tropical tropopause derived from radiosonde data and NCEP reanalyses. *J. Geophys. Res. Atmos.*, 2000, **105**, 15509–15523.
34. Dethof, A., O'Neill, A., Slingo, J. and Smit, H., A mechanism for moistening the lower stratosphere involving the Asian summer monsoon. *Q. J. R. Meteorol. Soc.*, 1999, **125**, 1079–1106.
35. Norton, W. A., Tropical wave driving of the annual cycle in tropical tropopause temperatures. Part II: model results. *J. Atmos. Sci.*, 2006, **63**, 1420–1431.
36. Meenu, S., Rajeev, K., Parameswaran, K. and Nair, A. K. M., Regional distribution of deep clouds and cloud top altitudes over the Indian subcontinent and the surrounding oceans. *J. Geophys. Res.-Atmos.*, 2010, **115**, 1–12.
37. Dey, S., Nishant, N., Sengupta, K. and Ghosh, S., Cloud climatology over the oceanic regions adjacent to the Indian Subcontinent: inter-comparison between passive and active sensors. *Int. J. Remote Sens.*, 2015, **36**, 899–916.
38. Das, S. S., Jain, A. R., Kumar, K. K. and Rao, D. N., Diurnal variability of the tropical tropopause: Significance of VHF radar measurements. *Radio Sci.*, 2008, **43**, 1–14.
39. Sasi, M. N., Ramkumar, G. and Deepa, V., Nonmigrating diurnal tides in the troposphere and lower stratosphere over Gadanki (13.5°N, 79.2°E). *J. Geophys. Res. Atmos.*, 1998, **103**, 19485–19494.
40. Kishore, P., Velicogna, I., Venkat Ratnam, M., Jiang, J. H. and Madhavi, G. N., Planetary waves in the upper stratosphere and lower mesosphere during 2009 Arctic major stratospheric warming. *Ann. Geophys.*, 2012, **30**, 1529–1538.
41. Coughlin, K. and Tung, K. K., Eleven-year solar cycle signal throughout the lower atmosphere. *J. Geophys. Res. Atmos.*, 2004, **109**, 1–7.
42. Huang, B., Hu, Z. Z., Kinter, J. L., Wu, Z. and Kumar, A., Connection of stratospheric QBO with global atmospheric general circulation and tropical SST. Part I: Methodology and composite life cycle. *Climate Dyn.*, 2012, **38**, 1–23.
43. Suneeth, K. V., Das, S. S. and Das, S. K., Diurnal variability of the global tropical tropopause: results inferred from COSMIC observations. *Climate Dyn.*, 2017, **49**, 3277–3292.
44. Shepherd, T. G., Issues in stratosphere-troposphere coupling. *J. Meteorol. Soc. Jpn.*, 2002, **80**, 769–792.

ACKNOWLEDGEMENTS. INSAT-3D data used in the present study were obtained from the MOSDAC. We thank the NARL staff for their dedicated efforts in launching radiosondes. Radiosonde data used in the present study were obtained from the TTD experiments conducted as a part of CAWSES India Phase II programme. A.H.K. thanks the Science and Engineering Research Board, Department of Science and Technology, Government of India for the National Post-Doctoral Fellowship (PDF/2017/001785).

Received 8 August 2017; revised accepted 10 May 2019

doi: 10.18520/cs/v117/i11/1813-1827